

SWIFT XRT OBSERVATIONS OF X-RAY FLARES IN GRB AFTERGLOWS

David N. Burrows¹, P. Romano², O. Godet³, A. Falcone¹, C. Pagani^{1,2}, G. Cusumano⁴, S. Campana², G. Chincarini^{2,5}, J. E. Hill^{1,6}, P. Giommi⁷, M. R. Goad³, J. A. Kennea¹, S. Kobayashi^{1,8}, P. Mészáros¹, J. A. Nousek¹, J. P. Osborne³, P. T. O'Brien³, K. L. Page³, G. Tagliaferri², B. Zhang⁹, and the Swift XRT team¹⁰

¹Department of Astronomy & Astrophysics, 525 Davey Lab., Penn. State University, University Park, PA 16802, USA

²INAF-Osservatorio Astronomico di Brera, Via Bianchi 46, 23807 Merate, Italy

³Department of Physics and Astronomy, University of Leicester, Leicester LE1 7RH, UK

⁴INAF-Istituto di Astrofisica Spaziale e Fisica Cosmica, Via Ugo La Malfa 153, 90146 Palermo, Italy

⁵Università degli studi di Milano-Bicocca, Dipartimento di Fisica, Piazza delle Scienze 3, I-20126 Milan, Italy

⁶NASA-Goddard Space Flight Center / Universities Space Research Association

⁷ASI Science Data Center, via Galileo Galilei, 00044 Frascati, Italy

⁸Astrophysics Research Institute, Liverpool John Moores University, Birkenhead CH41 1LD, UK

⁹Department of Physics, University of Nevada, Box 454002, Las Vegas, NV, 89154-4002, USA

ABSTRACT

The Swift XRT has been observing GRB afterglows since December 23, 2004. Three-quarters of these observations begin within 300 s of the burst onset, providing an unprecedented look at the behavior of X-ray emission from GRB afterglows in the first few hours after the burst. While most of the early afterglows have smoothly declining lightcurves, a substantial fraction has large X-ray flares on short time-scales. We suggest that these flares provide support for models with extended central engine activity producing late-time internal shocks.

Key words: GRBs; Swift; X-rays; afterglow.

1. INTRODUCTION

The Swift Explorer mission (Gehrels et al., 2004) was launched on November 20, 2004. It is detecting two bursts per week on average, and following these up with detailed optical/UV and X-ray observations. In 75% of the bursts, the spacecraft can slew immediately to the field and observations with the X-ray Telescope (XRT; Burrows et al., 2005a) begin within 5 minutes of the GRB trigger (in the remaining cases the source is too close to the Earth, Moon, or Sun and XRT observations are delayed). While early X-ray observations are available for a handful of previous bursts (e.g., see Piro et al., 2005), the large number of these observations made available by Swift is revolutionizing our knowledge base of early GRB X-ray afterglows. At the time of this writing (31 October 2005), the XRT has detected 67 X-ray afterglows

of GRBs (exceeding the total pre-Swift afterglow sample), 51 of which were observed within 300 s of the trigger.

Here we discuss the discovery of X-ray flares, commonly seen during the first several hours after the burst. These flares are seen in approximately 50% of all GRBs, and cover a range of time-scales and intensities. This paper will highlight some of the key findings that led us to the conclusion that the flares are produced by extended central engine activity producing X-rays from internal shocks at times long after the cessation of hard X-ray/gamma-ray emission.

2. GRB 050406

Although in retrospect, the first flare observed by the XRT was probably in GRB 050219A (Tagliaferri et al., 2005; Goad et al., 2005), the first clear-cut example was GRB 050406 (Romano et al., 2005; Burrows et al., 2005b). The X-ray light curve of GRB 050406 is shown in Figure 1. There is a strong flare peaking at about 210 s after the BAT trigger, which rises above the underlying power-law decay by a factor of 6. The rapid power-law decay in the first 1000 s has a decay index of 1.58 ± 0.17 . At about 4400 s the light curve breaks to a flatter decay index of $0.50^{+0.14}_{-0.13}$ (Romano et al., 2005). When the underlying decay is subtracted, the flare itself peaks at 213 s and has rise/fall rates (expressed as power-law indices) of ± 6.8 . The flare can also be fitted as a Gaussian, in which case the width is $17.9^{+12.3}_{-4.6}$ s, and $\delta t/t_{peak} \sim 0.2 \ll 1$, where we take $\delta t = \text{FWHM of the Gaussian} = 42.2^{+29.0}_{-10.8}$ s.

The light curve of the flare can be obtained in two energy

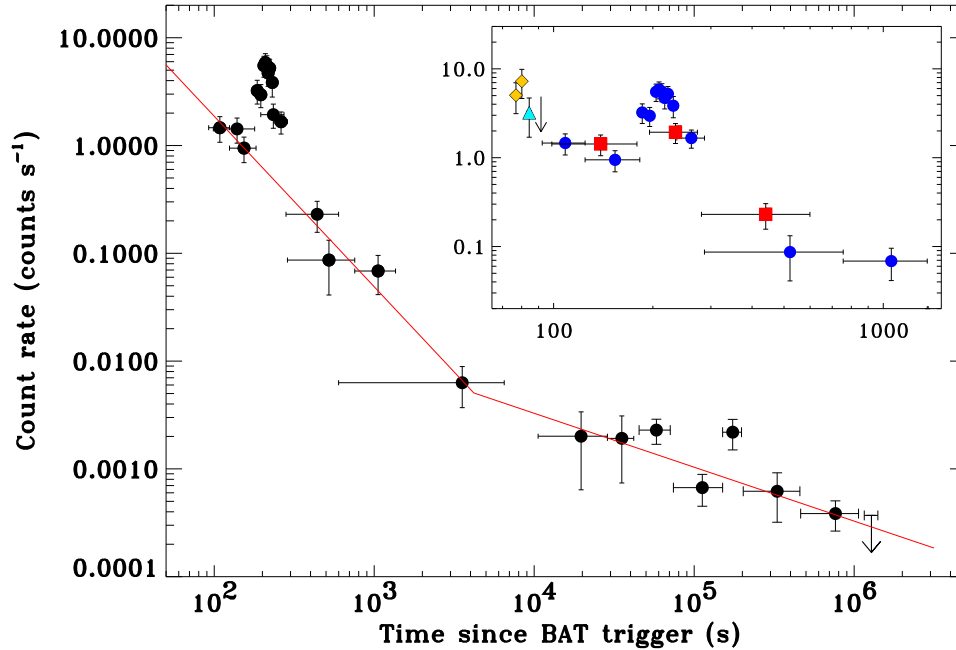


Figure 1. Background-subtracted X-ray light curve of GRB 050406 (0.2-10 keV). The red solid line shows the best-fit broken power-law model for the points excluding the flare at about 210 s. The inset shows details of the first 1000 s. Yellow diamonds are data taken in Photodiode (PD) mode, the cyan triangle is from the Image (IM) mode frame, the blue circles are from Windowed Timing (WT) mode data, and the red squares are Photon-Counting (PC) mode (see Hill et al., 2004). For details of the data processing and analysis, see Romano et al. (2005).

bands to allow a search for spectral variations. Figure 2 shows the light curve in soft and hard bands, as well as the ratio of the hard to soft bands. The flare begins in the hard band, softening significantly as it decays. This is similar to the behavior typically seen in the prompt gamma-ray emission from GRBs, and in particular, seen in the prompt emission from this burst.

To reiterate, the key features seen in this flare are:

- Underlying afterglow consistent with a single slope before and after the flare.
- Flare increases by factor of 6.
- $\delta t/t \ll 1$ for both the rising and falling sides of the flare.
- Flare softens as it progresses.

3. GRB 050421

The XRT observations of GRB 050421 show a large flare and a small flare superposed on a single power-law decay with a decay index of 3.1 ± 0.1 (Figure 3). Although not as well sampled as GRB 050406, primarily due to the extremely rapid rise and fall of this flare, the X-ray light curve can be well-modelled as a single power-law decay with two Gaussian flares superposed. The stronger flare peaks at 111 ± 2 s and has an extremely steep rise and

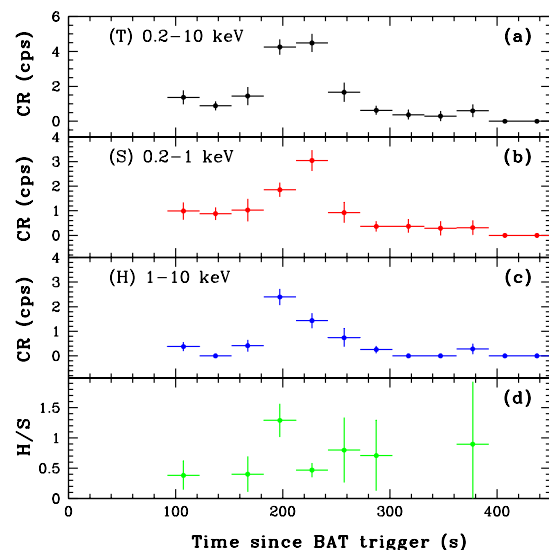


Figure 2. Background-subtracted X-ray light curves of the GRB 050406 flare. (a) Total intensity (0.2-10 keV). (b) Soft band (0.2-1.0 keV). (c) Hard band (1.0-10 keV). (d) Band ratio (H/S). Note that the hard band peaks before the soft band; this is also reflected in the band ratio, which is quite hard at the onset of the flare. For details of the data processing and analysis, see Romano et al. (2005).

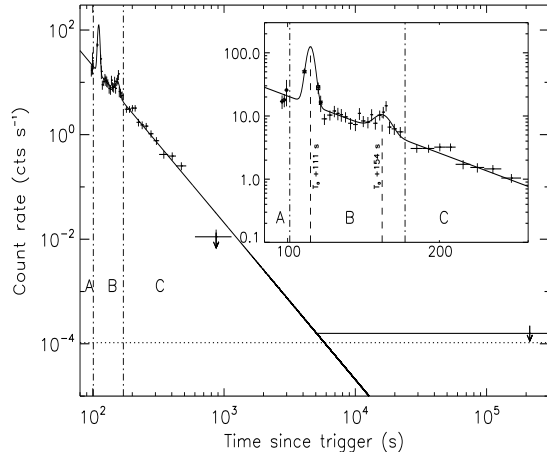


Figure 3. Background-subtracted X-ray light curve of GRB 050421 (0.3-10 keV). The solid line shows the best fit model, consisting of a power-law plus two Gaussian flares centered at 110 and 154 seconds post-burst. Data during time period A are in Photodiode (PD) mode (diamonds). Time period B has data in PD mode (square and star), and WT mode. Data in interval C are in PC mode. For details of the data processing and analysis, see Godet et al. (2005).

fall, with $\delta t/t \sim 0.07$ for both the rise and fall times, and increases by a factor of 4 above the underlying power-law decay (Godet et al., 2005).

Salient features of GRB 050421 include:

- Underlying afterglow consistent with a single slope before and after the flare.
- Flare increases by factor of ~ 4 .
- $\delta t/t \ll 1$ for both the rising and falling sides of the flare.

4. GRB 050502B

The largest flare seen to date occurred in the light curve of GRB 050502B (Falcone et al., 2005; Burrows et al., 2005b). The X-ray light curve of this burst is shown in Figure 4. The light curve has an enormous flare peaking at about 650 s post-burst, with late-time bumps at about 30,000 s and 700,000 s. The main flare is shown in more detail in Figure 5, where the underlying afterglow is indicated by a solid line, as are power-law fits to the rising and falling parts of the flare, which are extremely steep, with power-law indices of about 9.5. The fluence of the giant X-ray flare, $\sim 9 \times 10^{-7}$ ergs cm^{-2} , actually exceeds the fluence ($\sim 8 \times 10^{-7}$ ergs cm^{-2}) of the prompt gamma-ray burst detected by the Swift Burst Alert Telescope (Barthelmy et al., 2005a).

As in the case of GRB 050406, we have generated light curves in two energy bands for this burst, shown in Fig-

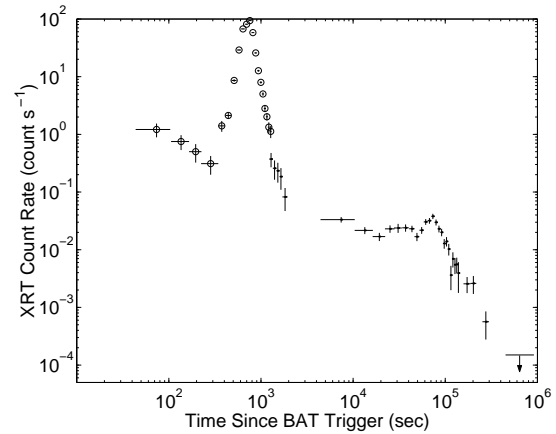


Figure 4. Background-subtracted X-ray light curve of GRB 050502B (0.2-10 keV). Open circles represent WT mode data and dots represent PC mode data. The latter were corrected for pile-up where necessary. For details of the data processing and analysis, see Falcone et al. (2005).

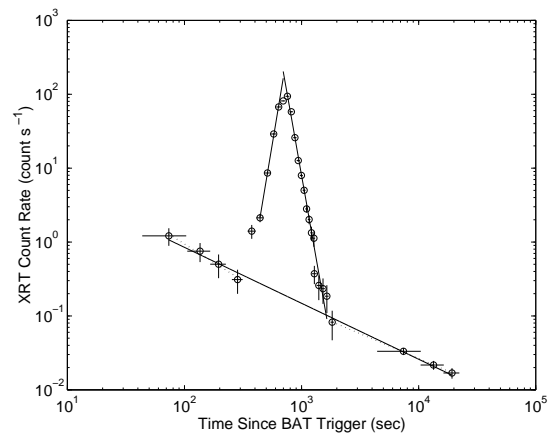


Figure 5. Background-subtracted X-ray light curve of the GRB 050502B flare (0.2-10 keV). The solid lines indicate the underlying afterglow (decay index of 0.8) and fits to the flare rise and decay. For details of the data processing and analysis, see Falcone et al. (2005).

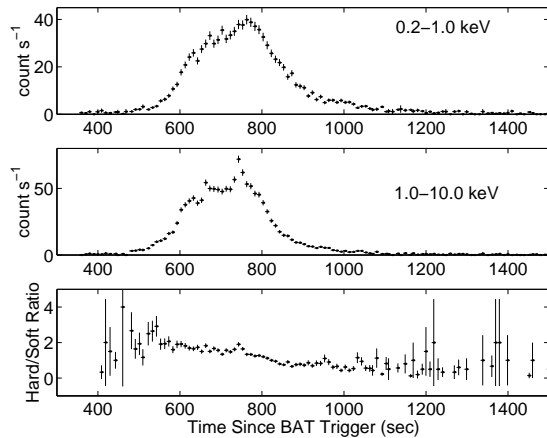


Figure 6. Background-subtracted X-ray light curves of the GRB 050502B flare. Top: Soft band (0.2-1.0 keV). Middle: Hard band (1.0 - 10 keV). Bottom: H/S band ratio. Like GRB 050406, the beginning of the flare is significantly harder than the preceding afterglow, and the flare softens as it evolves, eventually ending up with a band ratio similar to the pre- and post-flare afterglow. For details of the data processing and analysis, see Falcone et al. (2005).

ure 6. The flare is significantly harder than the pre- and post-flare afterglow, and softens gradually as it evolves, with the hard band decaying much faster than the soft band. We note that there is rapid variability in the hard band at about 750 s.

The key features of this flare are:

- Underlying afterglow consistent with a single slope before and after the flare.
- Flare increases by factor of 500.
- $\delta t/t < 1$ for both the rising and falling sides of the flare.
- $\delta t/t \ll 1$ for the spike at the peak of the hard band.
- Flare softens as it progresses.

5. GRB 050607

The X-ray light curve of GRB 050607 is shown in Figure 7. Two flares are superposed on an underlying power-law decay (index 0.58 ± 0.07 until about 12 ks post-burst) in the first 500 s post-burst. In this case, we do not measure the afterglow intensity before the first flare, which may already be in progress when the XRT begins collecting data. The BAT data points have been extrapolated into the XRT band using two different spectral models, showing that they are at least roughly consistent with the XRT flux at about 100 s.

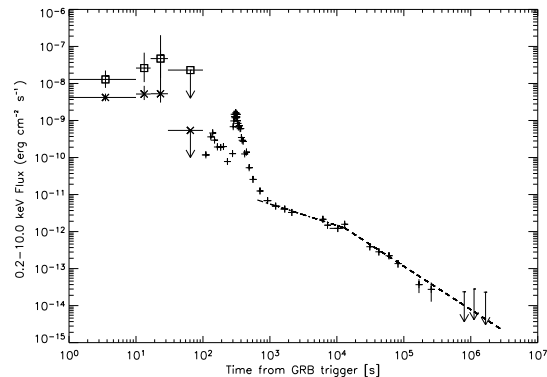


Figure 7. Background-subtracted X-ray light curve of GRB 050607 (0.2-10 keV). This light curve includes two different extrapolations of BAT data points into the XRT energy band (points before 100 s). The points after 100 s are XRT data, corrected for pile-up where necessary. The best-fit broken power-law is shown by the dashed and dash-dot lines. This light curve has two early flares. For details of the data processing and analysis, see Pagani et al. (2005).

The main flare, which peaks at about 310 s, has a total fluence about 16% of the BAT prompt fluence. The rising portion of this flare is extremely steep, with a power-law slope of about 16 when referred to the BAT trigger, or about 2.5 when referred to the beginning of the flare itself, and $\delta t/t \sim 0.2$. The decay following the flare is less steep; this flare is less symmetrical than the other examples presented here.

We have produced light curves in two energy bands to examine spectral variations during the flare (Figure 8). As in previous cases, the hard band rises faster than the soft band and also decays faster, resulting in an increase in hardness ratio at the beginning of the flare and a gradual decrease as the flare evolves and decays. Note that these statements are true for *both* flares.

Salient features of these flares include:

- Two flares in first 500 s.
- Main flare increases by factor of ~ 20 .
- $\delta t/t \ll 1$ for the rising side of the flares.
- $\delta t/t < 1$ for the falling side of the flares.
- Both flares soften as they progress.

6. GRB 050730

This remarkable light curve (Figure 9) shows at least three successive flares of comparable magnitude (factor of 3-4) and durations (~ 200 s). Furthermore, substantial flaring and variability continue in this light curve out to times of at least 35 ks in the observer's frame.

7. DISCUSSION

The flares discussed in the preceding sections have several features in common, which collectively point to an emission mechanism associated with internal shocks in the GRB jet:

- Rapid rise and fall times, with $\delta t/t_{peak} \ll 1$. It is very difficult to obtain rapid variability in the external shock, since the radiation physics of the shock results in decay time constants no faster than $\delta t/t_{peak} \sim 1$ (Ioka et al., 2005). Possible mechanisms associated with the internal shocks and jet for these rapid variations include extended central engine activity, anisotropic jets, or a jet comprised of many “mini-jets” (Ioka et al., 2005).
- Many light curves have evidence for the same afterglow intensity and slope before and after the flares (see Osborne et al., 2005, for a counterexample). This argues against energy injection into the external shock by the flare, as would be expected if the flare were associated with the external shock.
- Multiple early flares (at least 3 for GRB 050730) argue against one-shot explanations like the beginning of the afterglow.
- Large flux increases (factors of tens to hundreds) are incompatible with origins related to the Synchrotron Self-Compton mechanism in the reverse shock (Kobayashi et al., 2005).
- Flares typically soften as they progress. This is very reminiscent of the behavior of the prompt emission.

Our conclusion is that the most likely explanation, which seems to account for all of these observed features of the x-ray flares, is that they are caused by internal shocks similar to those that produce the prompt emission, but with lower resultant photon energies. The lower energies are a natural consequence of the late times (and corresponding large radii) at which these flares are observed.

This conclusion requires extended activity by the central engine at times long after the cessation of the prompt gamma-ray emission. This points in turn to a mechanism like fall-back of material into the new black hole whose formation caused the GRB, as discussed by MacFadyen, Woosley, & Heger (2001) and King et al. (2005).

More extensive discussions can be found in Nousek et al. (2005), Zhang et al. (2005), and Panaitescu et al. (2005).

8. GRB 050904

We now consider the case of GRB 050904, the highest redshift GRB found to date. The X-ray lightcurve of this

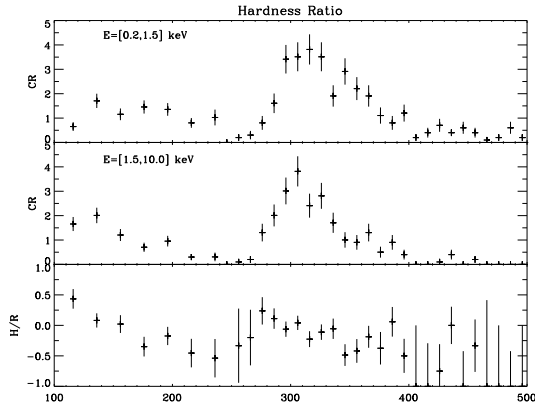


Figure 8. Background-subtracted X-ray light curves of GRB 050607. The top panel shows the soft (S) band light curve (0.2-1.5 keV in this case), the middle panel shows the hard (H) band (1.5 - 10 keV), and the bottom panel shows the hardness ratio, defined as $(H-S)/(H+S)$. For details of the data processing and analysis, see Pagani et al. (2005).

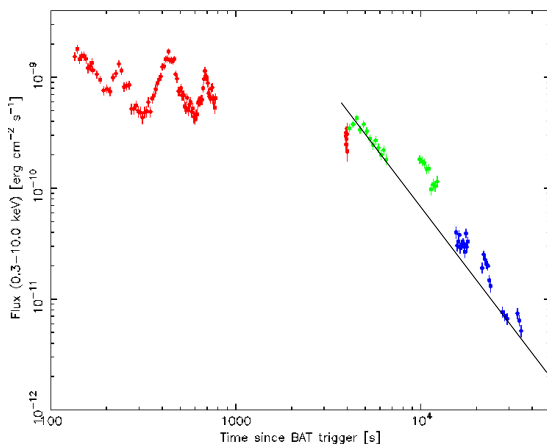


Figure 9. Background-subtracted X-ray light curve of GRB 050730 (0.3-10 keV). A possible underlying power-law decay after the first hour is indicated by the solid line. However, the variability throughout this light curve is so large that it is difficult (or impossible) to establish the level or slope of the afterglow contribution with certainty.

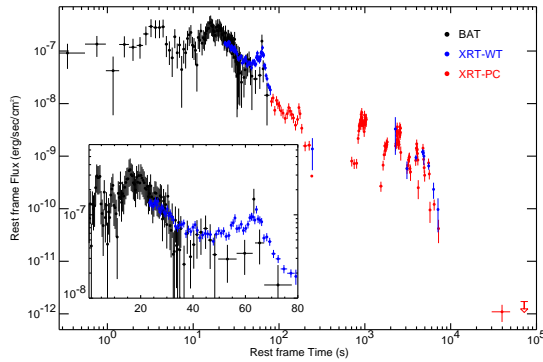


Figure 10. Background-subtracted X-ray light curve of GRB 050904, transformed into the rest frame for $z=6.29$. The plot shows the BAT light curve, extrapolated into the XRT energy range (black points, from 0-75 s) superposed on the XRT light curve (20-10,000 s). There is substantial overlap in this case between the BAT and XRT data points, which agree fairly well. For details of the data processing and analysis, see Cusumano et al. (2005).

burst is shown in Figure 10. The XRT light curve shows a spiky flare at about 65 s, with substantial fluctuations in count rate extending out to nearly 10 ks in the rest frame of the burst.

Soft and hard band light curves for GRB 050904 are shown in Figure 11. Unlike previous examples, the band ratio declines steadily during the first 80 s of the XRT data, but then remains low during the late-time variability, when the XRT count rate is varying by an order of magnitude or more.

This light curve exhibits several differences to those discussed in previous sections:

- Flaring seems to occur predominantly at much later times (thousands rather than hundreds of seconds).
- The late flares exhibit no spectral variability, in stark contrast to the flares discussed above.

It is not clear at this time whether the differences between the flaring activity in GRB 050904 and the bursts discussed above is related to the high redshift of GRB 050904, although it seems quite premature to suggest this on the basis of a single example. Observations of additional flares, including additional high redshift cases, will undoubtedly shed light on this over the next year.

9. GRB 050724

We conclude by briefly mentioning the short GRB 050724 (Figure 12). Unlike the short GRBs 050509B (Gehrels et al., 2005) and 050813 (Fox et al., 2005), which were very faint in X-rays and exhibited power-law decays until they disappeared, the X-ray light

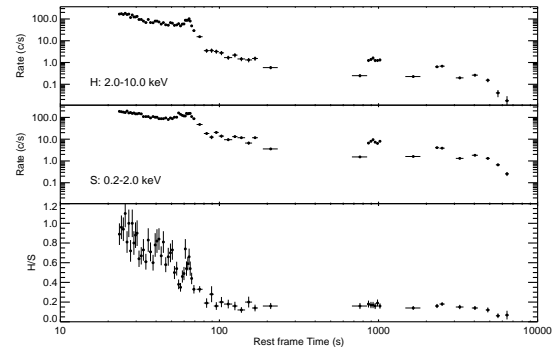


Figure 11. Background-subtracted X-ray light curves of GRB 050904, transformed into the rest frame for $z=6.29$. The upper panel shows the hard (H) band (2-10 keV in this case), the middle panel shows the soft (S) band (0.2-2 keV), and the lower panel shows the band ratio (H/S). For details of the data processing and analysis, see Cusumano et al. (2005).

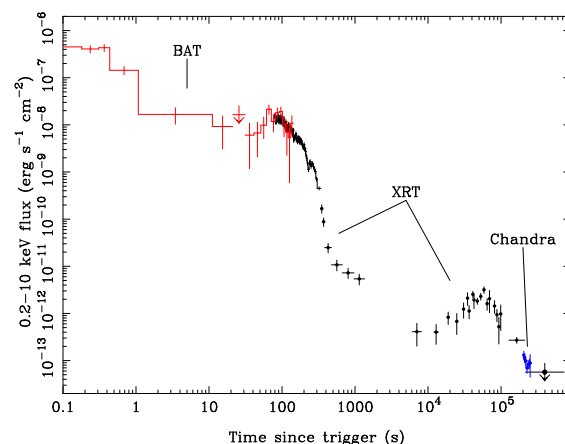


Figure 12. Background-subtracted X-ray light curve of GRB 050724, showing BAT data extrapolated into the XRT band, XRT data, and Chandra data. For details of the data processing and analysis, see Barthelmy et al. (2005b).

curve of GRB 050724 is bright, complex, and has several flare-like features. The optical and X-ray afterglows of this burst are clearly associated with an elliptical galaxy (Barthelmy et al., 2005b), making it very likely that the GRB was the result of a compact object merger. How then, in the rarified environment of a compact binary system in the outskirts of an elliptical galaxy, can the central engine produce flares and bumps at the late times seen in this light curve? One possibility is a neutron star-black hole merger. It is possible in such a system, given the right initial conditions, for the black hole to shred the neutron star, resulting in a lengthy period of in-fall into the black hole from the shredded remnants of the neutron star.

10. CONCLUSIONS

Observations of GRBs by the Swift XRT have shown that flaring is very common in X-ray light curves of GRBs and their afterglows. It seems likely that these flares result from extended central engine activity, pointing toward a much longer period of activity than expected on the basis of gamma-ray observations of prompt emission. Further progress in this area will undoubtedly result from statistical studies now underway of the properties of flares as an ensemble. Ultimately, we expect these observational results to lead to improved theoretical models of black hole formation and GRB central engines.

ACKNOWLEDGMENTS

This work is supported at Penn State by NASA contract NAS5-00136; at the University of Leicester by the Particle Physics and Astronomy Research Council under grant numbers PPA/G/S/00524 and PPA/Z/S/2003/00507; and at OAB by funding from ASI under grant number I/R/039/04.

REFERENCES

- Barthelmy, S., et al. 2005a, *Space Science Rev.*, in press (astro-ph/0507410)
- Barthelmy, S., et al. 2005b, *Nature*, in press
- Burrows, D. N., et al. 2005a, *Space Science Rev.*, in press (astro-ph/0508071)
- Burrows, D. N., et al. 2005b, *Science*, 309, 1833
- Cusumano, G., et al. 2005, *Nature*, submitted (astro-ph/0509737)
- Falcone, A., et al. 2005, *ApJ*, submitted
- Fox, D., et al. 2005, in preparation
- Gehrels, N., et al. 2004, *ApJ*, 611, 1005
- Gehrels, N., et al. 2005, *Nature*, 437, 851
- Goad, M., et al. 2005, *A&A*, submitted
- Godet, O., et al. 2005, *A&A*, submitted
- Hill, J. E., et al. 2004, *Proc. SPIE*, 5165, 217
- Ioka, K., Kobayashi, S., & Zhang, B. 2005, *ApJ*, 631, 429
- King, A., *ApJ*, 630, L113
- Kobayashi, S., Zhang, B., Mészáros, P., & Burrows, D. N. 2005, *ApJ*, submitted, (astro-ph/0506157)
- MacFadyen, A. I., Woosley, S. E., & Heger, A., *ApJ*, 550, 410
- Nousek, J. A., et al. 2005, *ApJ*, submitted (astro-ph/0508332)
- Osborne, J. P., et al. 2005, in preparation
- Pagani, C., et al. 2005, *ApJ*, submitted
- Panaitescu, A., et al. 2005, *MNRAS*, submitted (astro-ph/0508340)
- Piro, L., et al. 2005, *ApJ*, 623, 314
- Romano, P., et al. 2005, *A&A*, submitted
- Tagliaferri, G., et al. 2005, *Nature*, 436, 985
- Zhang, B., et al. 2005, *ApJ*, submitted (astro-ph/0508321)